United States Geological Survey

National Earthquake Hazard Reduction Plan

External Grants Program Announcement G11AS20009

Award Number: G12AP20086

Final Technical Report

Empirical Hazard Curve Assessment Using the Precarious Rock Archive

Glenn Biasi[1] and John Anderson[2]

University of Nevada Reno

Seismological Laboratory MS 0174

Reno, NV 89557

[1]Tel.: (775) 784-4576, Fax: 775-784-4165,

Email: glenn@seismo.unr.edu

[2]Tel.: (775) 784-1954, Fax: 775-784-4165,

Email: jga@seismo.unr.edu

Award Period: April 1, 2011 - December 31, 2013

Abstract

Precariously balanced rocks (PBRs) in southern California provide unexceeded bounds on ground motion during the time they have been in their present configuration. For many PBRs this time is at least thousands of years – much longer than any instrumental record at a point. Past studies of PBRs in California have focused on special collections of a few to perhaps tens of rocks. We employ a quantitative 2-D method to increase the number of quantitative measurements by over an order of magnitude. Rock survival as a function of distance from active faults provides an empirical ground motion prediction relation that can be compared to modern strong-motion derived estimates. Rock dynamic toppling accelerations are plotted in two views. In the first we plot rock versus distance to the nearest active fault, using the fault base of the 2008 National Seismic Hazard Map. A general pattern indicating increasing ground motion with decreasing distance is clear in this view. However, interpretation is difficult because rocks can be expected to survive longer near low slip rate faults that may generate earthquakes only every few thousand years. A more informative view is obtained by plotting all rocks relative to their distances to the San Andreas fault (SAF). Because of its high slip rate and rate of large earthquakes, hazard from the SAF dominates the ground motion hazard curve. In this view PBRs are seen to be consistent with median ground motions for Mw 7.8 to Mw 8.0 earthquakes on hard rock sites. Significantly, they also suggest a bound on event-to-event ground motion variability that is quite low compared to the total variability (sigma) in ground motion prediction experiments. Small "single-station" sigma has been anticipated by researchers based on several lines of argument. The PBR data give the clearest proof to date. We estimate that the event sigma contribution to GMPE variability for SAF sources is less than about 0.2 in natural log units.

Introduction

The primary goals of this project are:

1. To compare available and new estimates of precarious rock overturning accelerations to predictions from main ground motion prediction equations and to the National Seismic Hazard Maps for southern California.
2. Explore the parametric space in which PBRs are likely to survive, including median GMPE values, uncertainties in fault rate and magnitude distribution.
3. Make results available for use and improvement of seismic hazard estimates in southern California.

We approach these goals by improvement and consolidation of precarious rock images, expanding the set of quantitative estimates of precarious rock fragility, and plotting dynamic overturning acceleration as a function of distance from active faults in southern California. Anderson et al. (2011) review the broader context and research priorities of the precarious rock community.

Precarious Rock Database

A major effort under this project was the consolidation of four major photo collections into a single management environment. This effort required substantially more work than anticipated primarily because of their sizes and difficulty of collating around individual rocks. Each of the collections contained 2,000 to 4,000 individual images. The primary goal to consolidate images from different collections onto a single set of rocks has only partially been achieved. The current archive includes 12,396 images tied to 2915 unique rock identifiers. The eventual number of actual precarious rocks will be somewhat smaller because photos of the same rock often exist in more than one of the collections. Locations have been entered for 1972 of the rock ids. Rocks used in this study are shown in Figure 1.

The main quantitative estimate of precarious rock fragility is its quasi-static overturning acceleration. This acceleration is just sufficient to topple a rock when applied for a time long compared to the dynamic response of the rock. From the geometry of the problem, the quasi-static toppling acceleration is equal to the force of gravity times the tangent of an angle between vertical through the rock center of mass and the point at the edge of the rock around which it would rotate to topple. This angle is known as alpha, following the notation of Housner (1963). In general precarious rocks will have at least two directions in which the rock might topple, and thus at least two alphas.

Static overturning acceleration estimates in the database come from four different methods. We briefly review them here. Field testing involves physically moving the rock. These tests normally measure the force required to just lift the rock from one rocking point. For logistical reasons field testing often develops an alpha estimate only in one direction (Anooshehpoor et al., 2004). Field test estimates are available for 33 rocks. The photogrammetric method consists of estimating rock geometry and alphas from a large set of photographs. The photos are taken from around a rock, normally with visually unique targets on the rock. Specialized software is used to detect targets and unique points on the rock and invert them for rock shape. Brune et al. (2011) found that alpha estimates from photogrammetry were sufficiently similar to results from field testing that they recommended using photogrammetry exclusively. This recommendation reflects in part the greater logistical ease of photogrammetry and in part the fact that testing disturbs the rock and could compromise its long-term survival. The archive includes 45 estimates using photogrammetric methods, 40 of which are on unique rocks. A third method for estimating alphas may be termed “professional estimation”. Physical examination of the rock in the field can give a much more complete view, especially of 3-D mass distribution as it affects overturning accelerations. Such estimates have been developed for 62 rocks.

The last of our methods to estimate static overturning acceleration assumes that rocks can be represented by their 2-D views in suitably aligned photographs (Figure 2). The best views are usually taken from sufficient distance that the two rocking points and a good rock profile can be seen together. Alpha estimates are developed by marking the rocking points, then estimating the center of gravity from an outline of the rock (Figure 2). Applying this method requires 2-3 minutes using a Matlab application developed for the purpose. By its nature the 2-D analysis cannot consider 3-D qualities of a rock that

are not evident in the actual photo. Also, of necessity analyses must be made on the photos one has, and many rocks were not photographed with the 2-D method in mind. Thus the uncertainties using this approach are greater than they are for the first three methods. The Matlab interface was used, mainly by student analysts, to screen 7764 photographs, and to estimate alphas for 1901 images. One negative aspect of this per-photo view was that many views of the same rock could be developed, some with more favorable views than others. We address below how a final set of alphas was developed. We note in passing that no attempt by field surveys was made to comprehensively (or even casually) include less fragile (higher alpha) rocks. As a result nothing should be inferred from the declining density in alpha distributions above 30 degrees. In the reviewed alpha set there are 669 two-dimensional estimates.

A complete review of alpha estimates was conducted one rock at a time to increase confidence in the interpreted values. To do the review we first had to gather photos from separate collections and gather them around individual rocks. More remains to be done, but support under this project for archive organization made the review possible. For each rock we gathered views and rock parameters onto a simple web page (Figure 3). This made it possible to see all views together and to evaluate each estimate. Pedestal heights were estimated for all rocks. For each alpha estimate we determined whether the view angle and circumstances of the rock were appropriate for an alpha estimate. We then selected where necessary among the estimates. Field test results were given priority, followed by 3-D photogrammetric estimates, professional estimates, and then 2-D estimates. In addition to a best estimate, any valid alternatives were marked and retained. This allows us to use the database to compare alpha values among methods. Rocks shown in Figure 1 are the reviewed subset.

Summing up, we have useful static overturning acceleration estimates at 741 locations in southern California. Of the preferred estimates, 664 are from 2-D photographic analysis, 34 are from photogrammetry, and 32 are from field testing. We use single best reviewed estimates for analysis of ground motion constraints.

Fault Database

As a reference fault database we used the faults of the 2008 National Seismic Hazard Map (Figure 1; http://geohazards.usgs.gov/cfusion/hazfaults_search). Use of this fault database ensures the most direct comparison of PBR predictions to NEHRP objectives. This database includes the fault name, location, dip, slip sense, slip rate, and magnitudes of potential earthquakes hosted on the fault based on two leading magnitude-area regressions. Fault locations are expressed as piece-wise linear sections between latitude-longitude pairs. A Matlab routine was written to measure the shortest distance from each rock to each fault, including a criteria to detect whether the shortest distance is off the end of a fault.

The majority of active faults in the project area have a strike-slip sense of motion. Faults with the highest slip rates include the San Andreas and San Jacinto. A notable band of precarious rocks between the San Jacinto and Elsinore faults (Figure 1) has been

described by Brune et al. (2004). These rocks were noted to be inconsistent with the 1997 NSHM predictions and important "ground truth" data on which to evaluate ground motion expectations especially for ground motion variability.

Site Conditions at Precarious Rock Sites

Precarious rocks are, by their nature, sited on resistant rock pedestals. Lithologically sites with granite at the surface will have granite to a significant depth below them. This places the typical PBR site among the stiffest, and thus the lowest expected ground motions, of anywhere in Southern California. Several direct measurements of site conditions have been made at PBRs and PBR analog sites. Stirling et al. (2002) measured site amplifications at PBR sites relative to permanent seismic network stations of the Southern California Seismic Network. At the Lovejoy Buttes and Piute Buttes PBR sites, 15 and 20 km, respectively, from the San Andreas fault, they found relative deamplification below 4 Hz and a small amplification at higher frequencies. Their results indicated that there was little difference between PBR sites and site conditions of 760 m/s (NEHRP B-C site class boundary) assumed by the National Seismic Hazard Map.

The other two methods of measuring relevant site conditions use surface exploration techniques along horizontal profiles. Such profiles are generally chosen to minimize topography, and thus often are in locations with thin soil layers that are not present under the rock outcrop itself. Louie et al. (2010) used the Refraction Micro-tremor method at 13 PBR sites (Table 1; Figure 4). They also found high Vs30 in the granitic sections of their lines, in the range of 600-900 m/sec. If the high-velocity asymptotes of the velocity profiles beneath these profiles are interpreted as native granite velocities (Figure 4), all site velocities would be at or above 760 m/s. More recently Vs30 was estimated at 124 strong-motion sites in southern California (Yong et al., 2013). Of these, 24 sites had sites with Vs30>760 m/s, and photographs show that most of these were in granitic basement terrains favorable to development of PBRs. Yong et al. (2013) sites in granitic terrains showed shear-wave velocities the granites themselves (i.e., the subsoil layer velocities) closer to 1000 m/s. These studies together indicate that PBRs should be compared to current GMPEs assuming NEHRP B-C boundary (rock) conditions (Vs=760 m/s) or harder.

Relationship of Fault Slip Rate to Rock Survival

Expected rock survival probabilities relate to fault slip rate through the earthquake rate on the fault and through the uncertainty in ground motion prediction equations. The earthquake rate relates to slip rate through the expected slip per event. For example, a 2 meter average slip (roughly M7.2) could occur on a 20 mm/year fault once every 100 years, but on a 1 mm/year fault only once per 2000 years. A rock near these faults that has been precarious for 10000 years would experience 100 of the former events, but only 5 of the latter. The number of trials matters in comparing with the ground motion prediction equations through the uncertainty in the regressions (Figure 5). By construction half of earthquakes will cause ground motions higher than the median

value, and half will be below it. If a rock should just survive the median, then its survival in one earthquake is 50%. If instead the rock should survive, say, the +1σ level ground motion, then a smaller fraction of events (16%) will exceed this level – roughly once in 6 events. The width of the distribution determines how frequently to expect higher than median ground motions at any given value. For an example point at Lovejoy Buttes near the Mojave segment of the San Andreas fault, 3-4 meter displacement events are expected every ~150 years based event recurrence from paleoseismic studies at Pallett Creek (Scharer et al., 2011) and representative geologic slip rates. PBRs that have been in their present state for 10,000 years would have experienced over 60 events and almost certainly have sampled the upper tail of the GMPE distribution. A rock that would topple at 0.4 g that has survived 10,000 years can be used to say that sigma is more likely to be between 0.2 and 0.3. If several such rocks have survived it would be very unlikely that sigma is even as large as 0.25. We will return to this point later.

Toppling Accelerations and Distance From Active Faults

Estimated dynamic overturning accelerations for all reviewed rocks are plotted versus distance from the nearest active fault in Figure 6. Dynamic overturning accelerations were found by Anooshehpoor et al. (1999) to be roughly 1.3*tan(alpha) based on shake-table testing. Points are color coded according to the slip rate of the nearest fault. Red and magenta can be considered high slip-rate faults, with rates of >10 mm/yr and 3-10 mm/yr, respectively. Green and blue points are slowest faults, with rates of 0.5-1.0 and <0.5 mm/yr, respectively. Several observations may be made from the ensemble data. For all faults it is rare to find rocks more fragile than 0.2 g within 10 km of an active fault. An upper limit of ground shaking is suggested of between 0.3 and 0.4 g within 2 km of active faults. Ground motions apparently decrease rapidly with distance, such that it is relatively more common to find rocks fragile at 0.2g dynamic acceleration at 15 km from even the most active southern California faults.

Curves for median ground motions of the Abrahamson and Silva (2008; AS08) NGA ground motion prediction equation (GMPE) for Mw 6.8, 7.2, 7.6, and 8.0 are drawn on Figure 5 for comparison to dynamic estimates from the PBRs. A site Vs30 of 760 m/s has been assumed (site conditions are discussed in the next section). Comparing Figures 2 and 5 lead to an important conclusion of this project. Namely, median values of AS08 may be marginally consistent with long-term survival of known precarious rocks, but they would not be if ground motion sigma included the full range of the strong motion data set used to develop the GMPEs.

Figure 7 repeats only those points in Figure 6 that were developed by field methods – either physical testing, 3-D photo modeling, or field–based professional estimates. This more rigorous review can be seen to reduce the frequency with which rocks are found below median GMPE predictions. Nevertheless, rocks on a given median curve should, on average, be toppled approximately half the time in a single event, and have low probabilities of survival if exposed to many such events. From this we infer that a careful estimate of rock parameters is necessary, but perhaps not sufficient to constrain an empirical ground motion prediction.

In general the length of time that a rock has been in its precarious state is not known. However, based on correlations with cosmogenic ages and models of steady-state landscape evolution, pedestal height has been proposed as an approximate proxy for age (Brune et al., 2012, 2014). We developed estimates of pedestal height during our visual review of rock photos. This review also showed, however, for small pedestal heights, a single storm might suffice to create the fragility. Such a rock might be useful in a future earthquake, but does not usefully constrain past events. To use these concepts in development of an empirical ground motion prediction, we plotted a subset of alphas keeping only pedestals >50 cm in height (Figure 8). This screen left 277 rocks. Note that 2-D results are included. Most of the strong exceptions noted in Figures 6 and 7 are removed by the pedestal height screen. Comparison with Figure 7 indicates that many of the remaining exceptions are 2-D analyses.

Rock size also affects survival probability. The basic PBR model is a non-linear inverted pendulum. Large rocks have longer periods, and rocks taller than about 2 meters are less sensitive to ground motions because earthquakes do not generate sufficient amplitudes in that longer period. To evaluate this effect we remove from Figure 8 any rocks with a rocking arm length greater than 80 cm. The result, with 207 rocks, is plotted in Figure 9. The filter for rock size does remove some outliers, as expected.

Figures 8 and 9 bring out most clearly a contradiction by some rocks at short rock-to-fault distances in slow slip-rate faults. A review of the exceptions shows that they are concentrated along the Pinto Mountain and Cleghorn faults (4 and 2 rocks, respectively, of a total of 10 exceptions; Figure 1). Our interpretation of these exceptions, given that there are multiple rocks, is that these faults are inactive, or nearly so, or generating significant earthquakes with recurrence intervals $\sim 10^4$ years or longer.). For the Cleghorn fault UCERF3 also came to this conclusion, based on independent geologic mapping. The Pinto Mountain fault is aligned at nearly right angles to the emerging fault fabric of the Eastern California Shear Zone. Considering its geometry, the apparent aseismicity from PBR evidence is consistent with improved geological understanding of the fault.

To this point we have assumed that nearest active fault to a PBR controls the seismic hazard. For rocks near the San Andreas and San Jacinto faults this assumption seems secure, but elsewhere this assumption may not apply. As a test of whether the San Andreas fault controls seismic hazard relative to other lesser faults around it, we plotted dynamic toppling accelerations for reviewed rocks having pedestal heights >50 cm versus their distance from the fault (Figure 10). The result is perhaps the clearest evidence to date that PBRs are accurately recovering long-term seismic hazard from major faults in southern California. The estimated ground motions from the San Andreas fault effectively set a floor level for the hazard – a minimum that lower slip rate faults closer to the rock can only increase.

Ten rocks plot on Figure 10 are below the median prediction by Abrahamson and Silva (2008) for an M8 event, but seven of these plot at about the median of an M7.8

earthquake – the magnitude of the 1857 event. These seven are below the median for the M8 event by 0.03 g or less. Small deviations like this may be explained in many ways, as will be discussed subsequently. Thus, these points are not a fundamental exception to the well-defined floor to the hazard set by the majority of the points in Figure 10.

The toppling accelerations of the three rocks below the M7.6 median on Figure 10 are obtained from 2-D analyses. One at a distance of 12.0 km from the SAF can be seen in associated photographs to have structure out of the plane of view that contributes to the discrepancy. The other two, both with discrepancies of 0.09 g come from rocks known by only a single photo. These few exceptional points are not unexpected in a data set of this size, especially given the limitations of the 2-D method.

A constant feature of the PBR dynamic toppling acceleration data is that ground motions materially greater than median predictions would contradict the survival of increasing numbers of rocks. This is perhaps the clearest evidence to date from southern California that inter-event variability (tau, τ) in ground motions is small. We illustrate these limits using the model by Abrahamson and Silva (2008). Other models (e.g. US models by Boore and Atkinson (2008), Campbell and Bozorgnia (2008, 2013), Chiou and Youngs (2008, 2013), Abrahamson et al. (2013), Boore et al., 2013)) are similar enough that, while the numbers may change slightly, the results will be very similar.

Figure 10 allows us to quantify the variability of ground motions from the San Andreas fault. The width of the region above the median ground motion predictions and below the majority of data is an expression of how far above the median that ground motions have been during the life of the PBRs – a few thousand to 10,000 years in most cases. From paleoseismic studies and models of the recent rupture history of the San Andreas fault (Biasi, 2013; Scharer et al., 2007; Biasi and Weldon, 2009) indicate that Mw 7.8 events such as occurred in 1857 have occurred every 300 to 500 years on the central SAF. Slightly larger events, near Mw 8.0, are also possible, but should be slightly less frequent. The dotted and dashed lines in Figure 8 are drawn at 130% of the median for Mw 7.8, and 120% for Mw 8.0. An exact value for tau (ref. Figure 5) would depend on the magnitude distribution and earthquake occurrence rate, but in either case the PBRs indicate that tau for earthquakes on the San Andreas fault is on the order of 0.2 in natural log units. In pursuing a more precise value of tau, some reduction in ground motions and some increase in variability may come from site conditions. PBR site conditions may be more consistent with hard rock sites, of NEHRP site class B or stiffer (Vs30 >1000 m/s, making tau slightly larger). Even so, systematic PBR survival argues that the variability (sigma) around the median is small. We will be working to improve this estimate in future work.

We have only briefly touched on explanations for apparently rocks that survive near higher rate faults. The simplest is just that the rock looks free to topple, but for reasons not visible, is in fact cemented or wedged in place. This condition should be rare in field-derived estimates, and we screened for this condition in manual reviews of the 2-D analyses, but it cannot be categorically excluded. In principle it is also possible that

ground motions are systematically polarized into an orientation orthogonal to the sensitive direction of the rocks. Some measurement uncertainty for alpha is present for all measurement methods, but many of the exceptions in Figure 10 are based on 2-D analyses that have more uncertainty because of mass distribution not visible in the view of the photo. Finally, some rocks may have become precarious some time after the most recent large event. Screening by requiring a pedestal height >50 cm mitigates this issue, but cannot remove it entirely.

Discussion

We find that the general shape of GMPEs developed from strong motion recordings is consistent with survival of PBRs as a function of distance from active faults. On the other hand, we find that median predicted ground motions are barely consistent with the PBR data in southern California when PBR survival is predicted by distance to the nearest active fault.

A much stronger consistency is observed when rock dynamic toppling accelerations are plotted versus distance from the fault that dominates hazard, in this case, the San Andreas fault. PBRs are seen to be consistent with median ground motion predictions for the relevant magnitude events on the SAF. A perhaps more significant finding is that event variability can also be estimated, and is found to be small, on the order of 0.2 or less in natural log units. Low values of variability have been anticipated based on smaller samples of the PBR data (Anderson and Brune, 1999), but Figure 10 gives the clearest and most quantitative view to date based on "single station" observations spanning thousands of years.

Anderson and Brune (1999) argued against the ergodic assumption, of using strong motion data collected in space as a proxy for data collected at a point over long time periods. Atkinson (2006), Rodriguez-Marek et al. (2013), Anderson and Uchiyama (2011), and Biran et al. (2014) among others have pursued estimates of reduced sigma, arguing that common path and site terms should not materially vary in time, such that only the source term (magnitude, directivity and stress drop, primarily) contribute to sigma. PBR data strongly vindicate this view.

An implication is that the US National Seismic Hazard Map, to the extent that it utilizes larger values of total sigma than the value of tau that is implied by the PBRs, will tend to systematically overestimate the seismic hazard from southern California's main active faults on hard rock sites. The motivation for incorporating the total uncertainty due to the site condition into these maps is, of course, that the site condition is not known in general, so that a smaller, site-specific sigma will not suit the general user. The PBR sites represent a unique set of points, at which the site condition is uniformly good quality very hard rock. This level of quality control is not possible elsewhere, and thus reducing the variability at other sites may not be good policy unless the full effect of this variability is incorporated into the design process in every instance where the hazard from the US maps is utilized.

Bibliography

Results are being adapted for submission to the Bulletin of the Seismological Society of America.

References

Abrahamson, N. A., W. J. Silva, and R. Kamai (2013). Update of the AS08 ground motion prediction equations based on the NGA-West2 data set, *Pacific Earthquake Engineering Research Center Report 2013/04,* 174 pp.

Abrahamson, N. and W. Silva (2008). Summary of the Abrahamson and Silva NGA ground motion relations. *Earthquake Spectra*, 24(S1), 67-97.

Anderson, J. G., J. N. Brune, G. Biasi, A. Anooshehpoor, and M. D. Purvance (2011). Workshop report: Applications of precarious rocks and related fragile geological features to U. S. National Hazard Maps, *Seismological Research Letters, 82,* 431-441.

Anderson, J. G., and J. N. Brune (1999). Probabilistic seismic hazard assessment without the ergodic assumption, *Seismol. Res. Lett.* 70, 19–28.

Anderson, J. G., and Y. Uchiyama (2011). A methodology to improve ground-motion prediction equations by including path corrections, *Bull. Seismol. Soc. Am.* 101, 1822–1846.

Anooshehpoor, R., J. N. Brune, and Y. Zeng (2004). Methodology for obtaining constraints on ground motion from precariously balanced rocks, *Bulletin of the Seismological Society of America, 94*, 285–303.

Atkinson, G. M. (2006). Single-station sigma, *Bull. Seismol. Soc. Am.* **96,** 446–455.

Biasi, G. P. (2013). Appendix H – Maximum likelihood recurrence intervals for California paleoseismic sites, *U. S. Geological Survey*, *Open-File Report 2013-1165, Appendix H*: 25pp.

Biasi, G. and R. J. Weldon (2009). San Andreas Fault Rupture Scenarios From Multiple Paleoseismic Records: "Stringing Pearls", *Bulletin of the Seismological Society of America (BSSA)*, 99, 471-498.

Boore, D. M., J. P. Stewart, E. Seyhan, and G. M. Atkinson (2013). NGA-West 2 Equations for Predicting PGA, PGV, and 5%-Damped PSA for Shallow Crustal Earthquakes: *Earthquake Spectra*.

Boore, D. M. and G. M. Atkinson (2008). Ground-motion prediction equations for the average horizontal component of PGA, PGV, and 5%-damped PSA at spectral periods between 0.01 s and 10 s, Earthquake Spectra 24, 99-138.

Brune, J. N., A. Anooshehpoor, and M. D. Purvance (2006). Band of precariously balanced bocks between the Elsinore and San Jacinto, California, fault zones: constraints on ground motion for large earthquakes, *Geology* 34, 137–140.

Brune, J. N., R. Brune, G. P. Biasi, R. Anooshehpoor, and M. D. Purvance (2011). Accuracy of non-destructive testing of PBRs to estimate fragilities, Southern California Earthquake Center 2011 Annual Meeting Proceedings, B-080.

Brune, R., Brune, J. N., and Grant-Ludwig, L. (2014). Preliminary precariously balanced rock (PBR) age dates based on various models of erosion, *Seismological Research Letters, 85,* 544.

Brune, R. J., L. Grant-Ludwig, K. Kendrick, and J. N. Brune (2012). Geomorphic erosional models for estimating ages of precariously balanced rocks from cosmogenic isotope data, Southern California Earthquake Center 2012 Annual Meeting Proceedings, Poster 025.

Campbell, K. W., and Y. Bozorgnia, (2013). NGA-West2 Campbell-Bozorgnia Ground Motion Model for the Horizontal Components of PGA, PGV, and 5%-Damped Elastic Pseudo-Acceleration

Response Spectra for Periods Ranging from 0.01 to 10 sec, Pacific Earthquake Engineering Research center, PEER 2013/06.

Campbell, K. W. and Y. Bozorgnia (2008). NGA ground motion models for the geometric mean horizontal component of PGA, PGV, PGD, and 5%-damped linear elastic response spectra for periods ranging from 0.01 to 10 s., *Earthquake Spectra*, 24(S1), 139-172.

Chiou, B., and R. Youngs, (2013). Update of the Chiou and Youngs NGA Ground Motion Model for Average Horizontal Component of Peak Ground Motion and Response Spectra, Pacific Earthquake Engineering Research center, PEER 2013/07.

Chiou, B. S.-J. and Robert R. Youngs (2008). An NGA Model for the Average Horizontal Component of Peak Ground Motion and Response Spectra, Earthquake Spectra 24, 173-215.

Housner, G. W. (1963). The behavior of inverted pendulum structures during earthquakes. *Bulletin of the Seismological Society of America,* 53(2):403–417.

Louie, J. N., J.N. Brune, and S.K. Pullammanappallil, (2010). Estimates of Vs100 at sites of precariously balanced rocks, *Southern California Earthquake Center Annual Meeting,* I-073.

Rodriguez-Marek, A. F. Cotton, N. A. Abrahamson, S. Akkar, L. Al Atik, B. Edwards, G. A. Montalva, and H. M. Dawood (2013). A model for single-station standard deviation using data from various tectonic regions, *Bulletin of the Seismological Society of America, 103,* 3149-3163.

Scharer, K. M., G. P. Biasi, and R. J. Weldon II (2011). A reevaluation of the Pallett Creek earthquake chronology based on new AMS radiocarbon dates, San Andreas fault, California, *Journal of Geophysical Research, 116, B12111, doi: 10.1029/2010JB008099.*

Scharer, K. M., R. J. Weldon II, T. E. Fumal, and G. P. Biasi (2007). Paleoearthquakes on the southern San Andreas fault, Wrightwood, California, 3000 to 1500 B.C.: A new method for evaluating paleoseismic evidence and earthquake horizons, *Bulletin of the Seismological Society of America, 97*, 1054–1093, doi: 10.1785/0120060137.

Stirling, M., A. Anooshepoor, J.N. Brune, G.P. Biasi, and S.G. Wesnousky (2002). Assessment of the site conditions of precariously balanced rocks in the Mojave Desert, southern California, *Bulletin of the Seismological Society of America*, *92,* no. 6, 2139-2144.

Yagoda-Biran, G., J. G. Anderson, H. Miyake, and K. Koketsu (2014). Between-event uncertainty for "repeating earthquakes", Seismological Research Letters, 85, 544.

Yong, A. A. Martin, K. Stokoe, and J. Diehl (2013). ARRA-funded Vs30 measurements using multi-technique approach at strong motion stations in California and central-eastern United States, *USGS Open-File Report 2013-1102, 65 pp.*

Table 1. Locations of refraction microtremor Vs measurements and nearest precariously balanced rocks. Rock IDs are from the PBR archive. SAF: San Andreas fault; SJF: San Jacinto fault; EF: Elsinore fault.

Remi Lat	Remi Lon	# Rocks w/in 1 km	Distance to Remi line (km)*	Rock ID	Location	Km to SAF	Km to SJF	Km to EF
34.6534	-117.8518	2	0.150	R00968	Piute Butte	20.8	-	-
34.5894	-117.8482	3	0.396	R00970	Lovejoy Buttes	15.0	-	-
34.4163	-118.0920	35	0.254	R00967	Aliso Canyon	12.4	-	-
33.5928	-116.9242	3	0.102	R00051	Benton Road	-	13.6	16.4
33.5966	-116.9822	4	0.073	R00144	Stirrup Road	-	16.4	18.9

33.4815	-116.8491	26	0.095	R00015	Anza Hoodoo	-	19.6	5.4
33.5214	-116.9058	6	0.128	R01115	Round Top	-	19.3	6.2
33.2168	-116.4647	15	0.050	R00095	Tooth	-	16.7	17.0
33.9036	-116.9872	11	0.300	R00036	Beaumont South	15.9	-	-
33.7800	-117.1534	6	0.039	R00395	Menifee Nuevo	-	12.9	20.0
33.7892	-117.2404	28	0.060	R00993	Perris	-	18.0	15.9
33.8438	-117.3626	17	0.256	R01073	Mockingbird Tank	-	-	14.8
33.7997	-117.3946	13	0.215	R01211	Gavilan	-	-	9.3
33.8124	-116.6420	3	0.206	TramW	Tram Top west	14.7	-	-

* Many distances are overstated due to a to-be-resolved datum difference.

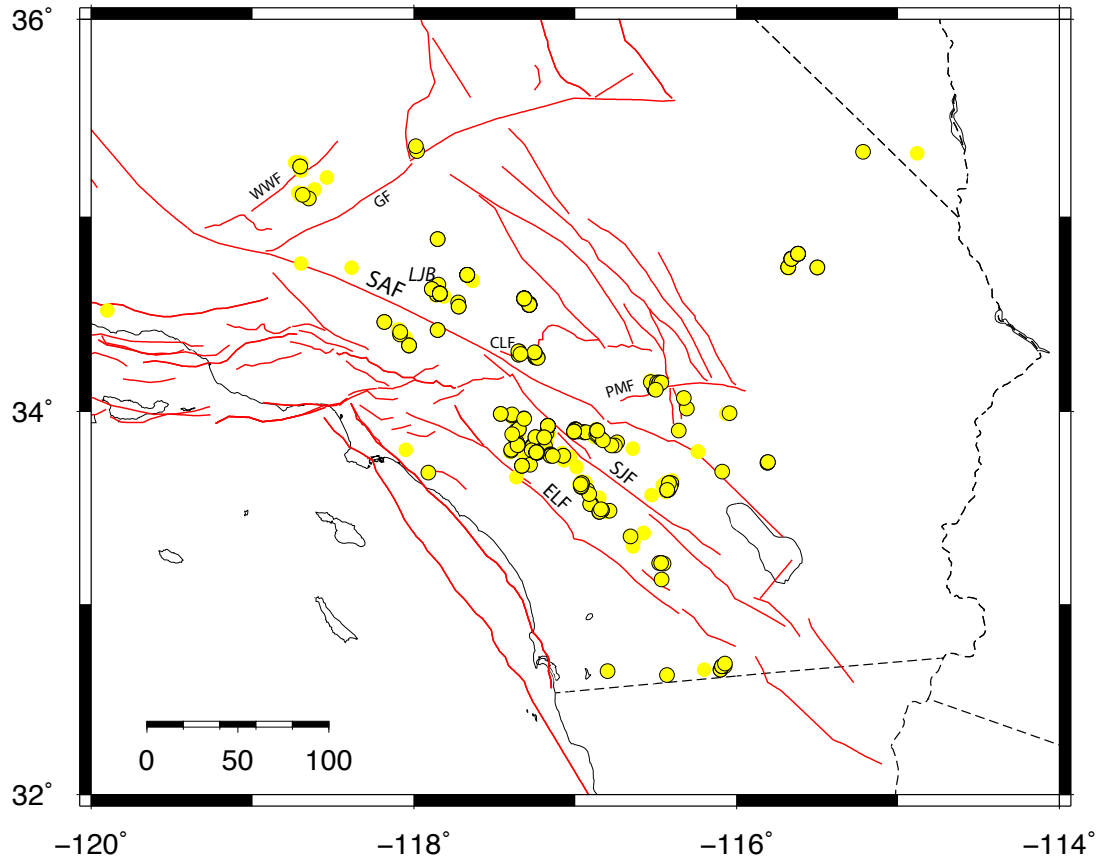

Figure 1. Precarious rock sites on a map of active faults of southern California. Faults are from the 2008 NSHM. Reviewed rocks with usable alphas in yellow. Black borders indicate pedestal heights >50 cm, used here as a proxy for rock age. SAF: San Andreas fault; WWF: White Wolf fault; GF: Garlock fault; CLF: Cleghorn fault; LJB: Lovejoy Buttes; PMF: Pinto Mountain fault; SJF: San Jacinto fault; ELF: Elsinore fault.

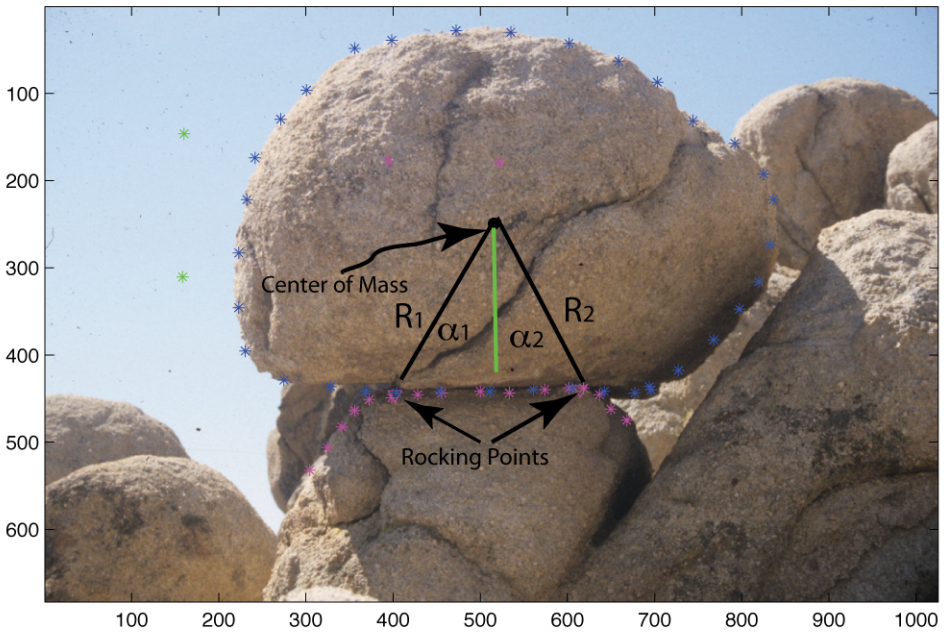

Figure 2. Example 2-D analysis in the Matlab interface for a rock on Alpine Buttes, about 16.5 km from the San Andreas fault. Horizontal and vertical coordinates are pixels. To estimate alphas, a graphical user interface is used to first mark the rocking points, then to outline the rock itself. The center of mass is calculated from the outline, and rocking angles are estimated. Where available, a vertical reference and absolute size are included. Alpha-1 and alpha-2 are 29.4 and 28.1 degrees, respectively, corresponding to a quasi-static toppling acceleration of 0.55g. A text file is generated with each analysis that preserves the fragility parameters and the digitized rock and pedestal outlines. These text files are then parsed and input into a customized relational database.

R4_00964, Aliso Canyon Rd, AC02

Basics

Rockid	Lat	Lon	Uncert (m)	Location	Alias(es)
R4_00964	34.4207	-118.0948	20.0000	Aliso Canyon Rd	AC02

Alphas, etc.

Esttype	imageid	alpha1	r1	alpha2	r2
2dh	1056	-999.0	-999.000	-999.0	-999.000
2dh	1057	-999.0	-999.000	-999.0	-999.000
2dh	1058	6.8	0.310	24.1	0.330
2dh	4424	-999.0	-999.000	-999.0	-999.000
2dh	4425	-999.0	-999.000	-999.0	-999.000
2dh	4426	-999.0	-999.000	-999.0	-999.000
ftest	1056	14.9	0.300	24.1	0.330
eye	1056	9.7	0.300	22.9	0.330

Images

1056 file://localhost/Users/glenn/Research/Precarious/PBR/Region4/ScannedSlides/AlisoCanyon/AlisoCanSanGMtns02-00/AlisoCanSanGMtns%2002-00%2013.jpg

1057 file://localhost/Users/glenn/Research/Precarious/PBR/Region4/ScannedSlides/AlisoCanyon/AlisoCanSanGMtns02-00/AlisoCanSanGMtns%2002-00%2014.jpg

1058 file://localhost/Users/glenn/Research/Precarious/PBR/Region4/ScannedSlides/AlisoCanyon/AlisoCanSanGMtns02-00/AlisoCanSanGMtns%2002-00%2015.jpg

4424 file://localhost/Users/glenn/Research/Precarious/PBR/Region4/RasoolsFiles/AlisoCanyonRd_7-25-2003/AC02/DSC05551.JPG

4425 file://localhost/Users/glenn/Research/Precarious/PBR/Region4/RasoolsFiles/AlisoCanyonRd_7-25-2003/AC02/DSC05552.JPG

4426 file://localhost/Users/glenn/Research/Precarious/PBR/Region4/RasoolsFiles/AlisoCanyonRd_7-25-2003/AC02/DSC05553.JPG

Image 1056

Image 1058

(continues on next page)

(other images not shown for brevity).

Figure 3. Web page for reviewing alternative alpha estimates. Rock R4_00964 is south of the San Andreas fault near the central Mojave reach of the fault. Each page includes a location block with basic parameters, a table of review documentation and alpha estimates, and a list of images available for the rock. The "imageid" is a unique number assigned to each image, for purposes of linking a view of the rock to subsequent analysis. By convention the first image of the set is assigned to estimates of type ftest, 3dpho, and eye. These estimates need a photo to anchor the observation, but have not come from a particular individual view. Six photos were available, three each from two collections. For some rocks images include associated movie files, the audio of which contains original field comments about the rock. Three estimates of alphas were developed for this rock (esttype column, Alphas, etc. table). When the Matlab 2D screening method is used and the photo is not suitable for analysis, the review esttype is still "2dh" to document that it was reviewed, but alphas are given non-data values (-999.0). Image 1058 was used for the 2D estimate. For this rock the three estimates are fairly similar, but field testing shows the rock is a bit more stable than it appears.

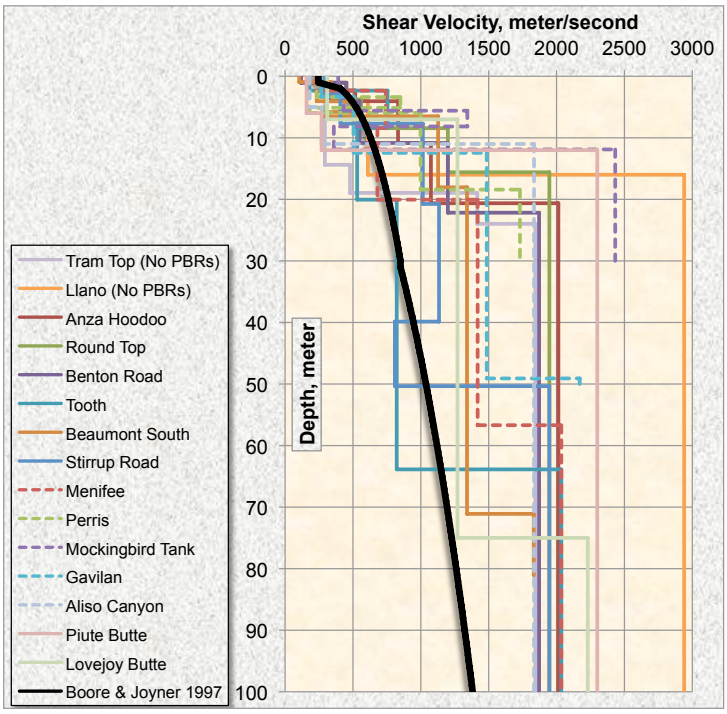

Figure 4. Shear-wave velocity profiles for 13 PBR sites and two granite sites not near PBRs. The model rock site velocity profile of Boore and Joyner (1997) is in black. Vs30 beneath the PBRs themselves are higher than the profiles shown because they are on rock outcrop with no thin or weathered cover. Figure from Louie et al. (2010).

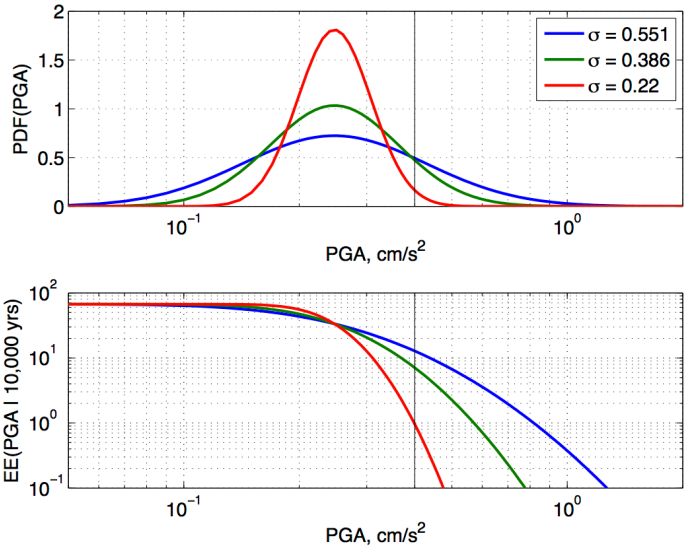

Figure 5: Illustration of the relationship between sigma and the probability of PBR survival. (upper) Distributions of expected ground motions from an M8.0 earthquake on the San Andreas fault at the Lovejoy Buttes site for the Campbell and Bozorgnia (2008) regression and three values of sigma. Vs30 is assumed to be 760 m/s. The vertical bar shows a representative overturning PGA of 0.4g. (lower) Hazard curves at Lovejoy Buttes for the same event. For the full GMPE uncertainty of σ = 0.551, approximately 12 events having accelerations sufficient to topple the rock are expected in a typical 10,000 year fragile phase of the rock. In addition, the site hazard curve is defined by these rare events, causing an inflation of seismic hazard at long return times. For the case σ=0.386, only 5-6 such events are expected. If σ=0.22, reflecting extremely small site and path sigma and limited source variability, only one event, on average, generates a demand comparable to rock capacity over the precarious phase of the rock.

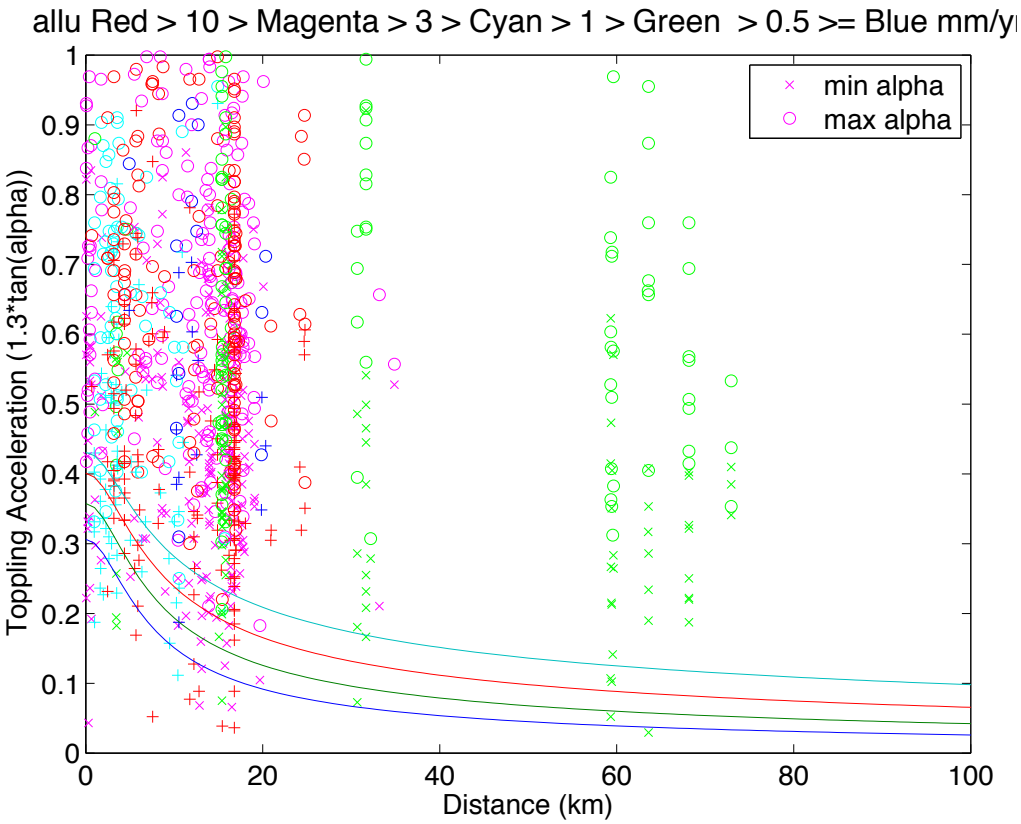

Figure 6. Summary results estimated dynamic toppling acceleration for all reviewed rocks as a function of distance from the nearest active fault. Minimum alpha estimates are shown with "+" or "x" and maximum alphas by "o" symbols, respectively. Colors indicate fault activity rates. Red: >10 mm/yr; magenta: 3-10 mm/yr; cyan: 1-3 mm/yr; green: 0.5-1.0 mm/yr; blue: <0.5 mm/yr. Smooth curves show median pseudospectral acceleration at 1 Hz (PSA(1.0)) from the Abrahamson and Silva (2008; "AS08") ground motion prediction equations increasing in order at values Mw 6.8, 7.2, 7.6, and 8.0. Red points come from the San Andreas and northern San Jacinto faults. Exceptional survivors may be seen for both faults. These are reviewed in more detail later in this report.

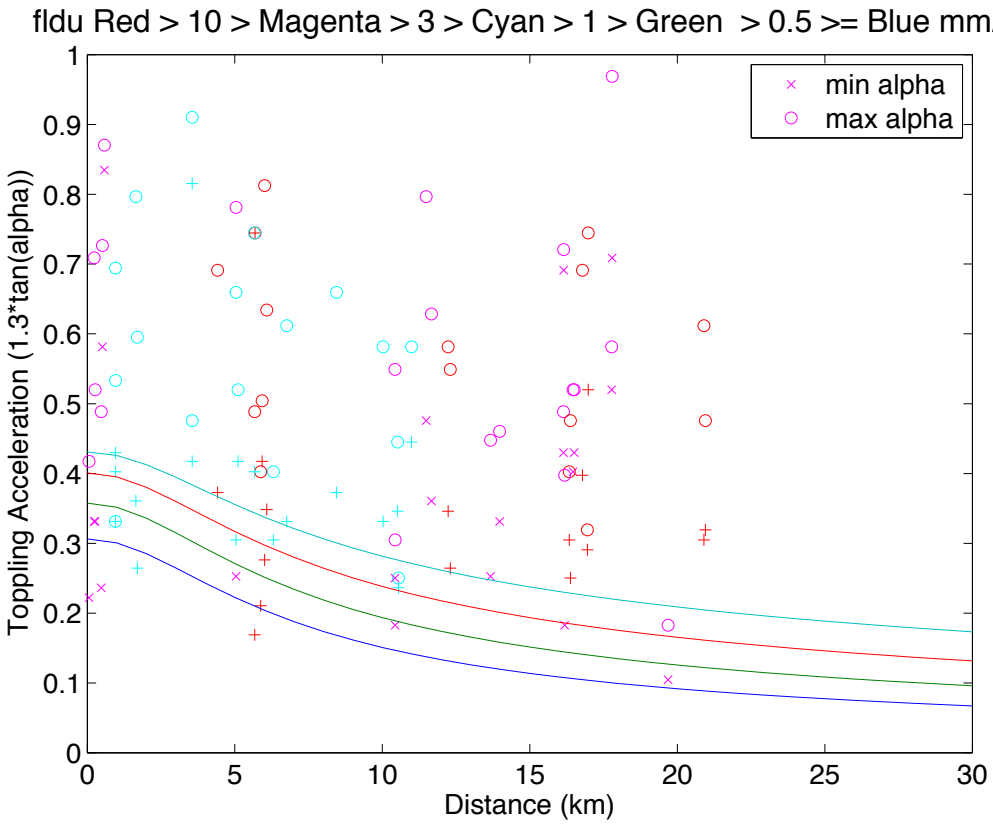

Figure 7. Plot of approximate dynamic toppling accelerations for alphas developed using field-based methods. These include physical testing, 3-D photogrammetry, and professional estimates. These are a subset of Figure 6 selecting only the estimates that are better reviewed and based on more complete 3-D information than can be considered in 2-D analysis. Symbols and symbol colors are as in Figure 5. Ground accelerations are median PSA(1.0) values for Mw = 6.8, 7.2, 7.6, and 8.0 from AS08. Predictably, alpha estimates from the more careful estimation methods include fewer apparent outliers. We note however that field-based methods did not necessarily focus on the most fragile rocks, so this subset should not be used to conclude that the 2-D data are incorrect.

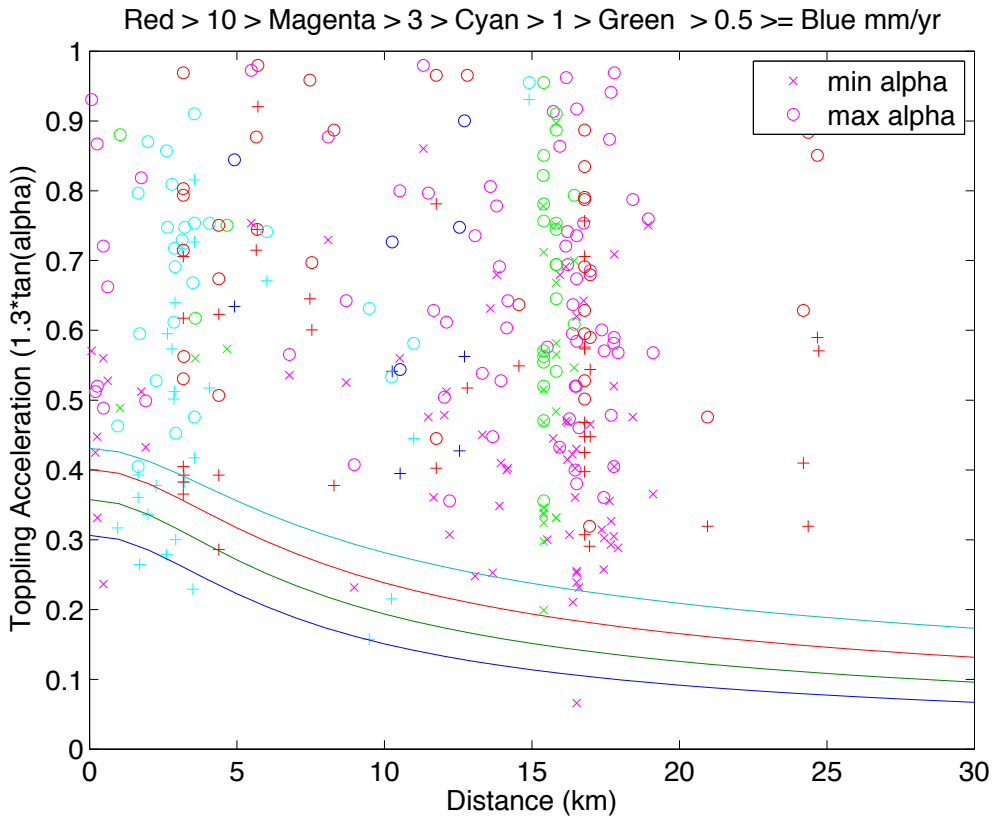

Figure 8. Subset of reviewed rocks with pedestal heights greater than 50 cm. Symbols and plotting as in the previous figure. 2-D estimates are included among the points plotted. Requiring a minimum pedestal height greater than 50 cm significantly improves agreement of PBR dynamic toppling acceleration estimates with median SA(1) predictions from AS08. A few survivors are indicated for high slip rate faults, but comparison with the previous figure indicates that they are mostly 2-D estimates.

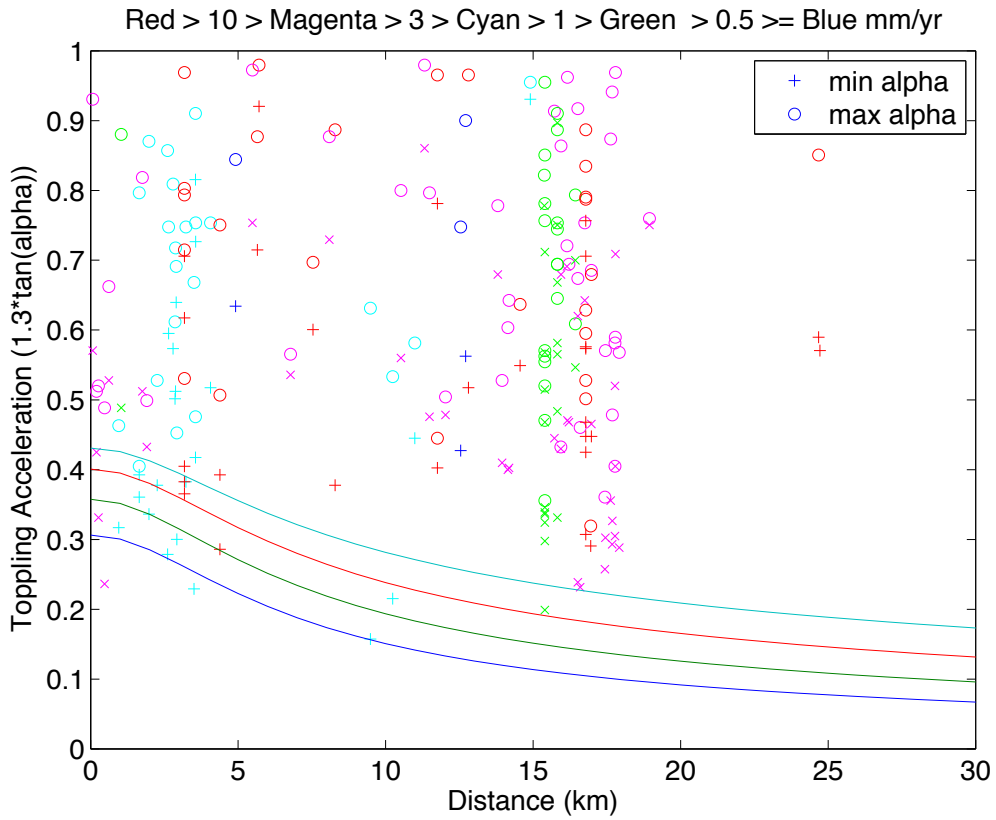

Figure 9. Subset with pedestal heights >50 cm and greatest rocking arm lengths less than 80 cm. Tall rocks are more stable at seismic frequencies. Comparison with Figure 8 shows that several apparently contradictory rocks are relatively large.

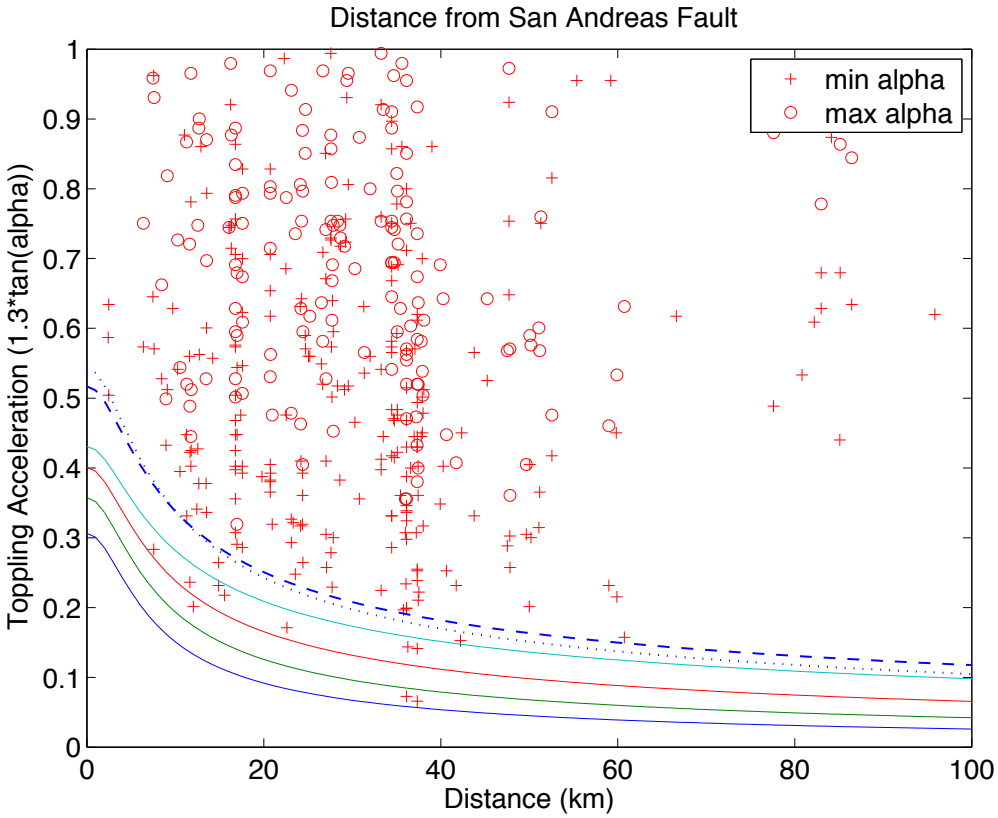

*Figure 10. Subset of reviewed with pedestal heights >50 cm plotted versus distance from the San Andreas fault. Because of its activity rate, the San Andreas fault sets a floor hazard above which other faults add according to their activity rates. Figure 8 shows the same rocks relative to the nearest active fault. A comparison of the two shows that the dominant hazard at long return times is from large events on the San Andreas fault. GMPE curves for Mw 6.8 (blue), 7.2 (green), 7.6 (red), and 8.0 (cyan) are shown for the AS08 GMPE. Two additional curves are shown to roughly estimate the implied upper ground motion above the medians. Blue dashed line = 1.20*M8.0 median; dotted line = 1.30*M7.8. Event-to-event variability in ground motion from large San Andreas fault events is strongly bounded by the PBR data.*